Amino Acids (2008) 35: 475–483
DOI 10.1007/s00726-007-0559-3
Printed in The Netherlands

Amino Acids

Beneficial impact of L-carnitine in liver: a study in a rat model of syndrome X

P. Rajasekar[1], **P. Viswanathan**[2], and **C. V. Anuradha**[1]

[1] Department of Biochemistry and Biotechnology, Faculty of Science, Annamalai University, Annamalai Nagar, Tamil Nadu, India
[2] Department of Pathology, Rajah Muthiah Medical College, Annamalai University, Annamalai Nagar, Tamil Nadu, India

Received January 31, 2007
Accepted April 23, 2007
Published online August 24, 2007;

Summary. The present study was designed to explore whether L-carnitine (CA) regulates insulin signaling and modulates the changes in liver in a well-characterized insulin resistant rat model. Adult male Wistar rats were divided into 4 groups. Groups I and IV animals received starch-based control diet, while groups II and III rats were fed a high fructose-diet (60 g/100 g). Groups III and IV animals additionally received CA (300 mg/kg/day i.p). After a period of 60 days hepatic tyrosine phosphorylation status was determined by assaying protein tyrosine phosphatase (PTP) and protein tyrosine kinase (PTK) activities. Oxidative damage was monitored by immunohistochemical localization of 4-hydroxynonenal (4-HNE), 3-nitrotyrosine (3-NT) and dinitrophenol (DNP)-protein adducts. In addition protein kinase C βII (PKC βII) expression, propidium iodide staining of isolated hepatocytes and histology of liver tissue were determined to examine liver integrity. Fructose-fed rats displayed reduced insulin action, increased expression of PKC βII, altered histology, fragmentation of hepatocyte nuclear DNA, and accumulation of oxidatively modified proteins. Simultaneous treatment with CA alleviated the abnormalities associated with fructose feeding. In summary the data suggest that elevated oxidative damage and PKC expression could in part induce insulin resistance and CA has beneficial impact on liver during insulin resistance with modulatory effects at the post-receptor level.

Keywords: Insulin resistance – Carnitine – Protein tyrosine kinase – Protein tyrosine phosphatase – Protein kinase C – Oxidative damage – Apoptosis

Introduction

Rat studies have demonstrated that high fructose feeding (60% of energy) produces a decline in insulin sensitivity in the liver and later in peripheral tissues and these rats form a convenient model of insulin resistance/syndrome X (Reaven, 1994). Alterations in the early steps of insulin action (Bezerra et al., 2000), decreased number of insulin receptors at the level of mRNA (Catena et al., 2003), reduction in the phosphorylation of pp185 (IRS-1/IRS-2) in liver (Ueno et al., 2000) are the findings in fructose-fed rats that contribute to insulin resistance. Sustained alteration in protein kinase C (PKC) activity has been reported in liver in this model (Donnelly et al., 1994) and PKC exerts strong inhibitory effects on the insulin receptor tyrosine kinase-autophosphorylation step (Bassienmaier et al., 1997). High fructose also facilitates oxidative damage (Faure et al., 1997). Miwa et al. (2000) demonstrated that lipid peroxidation products impair insulin secretion and post-receptor events of insulin action. Further, the excess amount of free radicals promotes apoptosis by causing lipid peroxidation, glutathione depletion, protein modification (Rauen et al., 1999), mitochondrial dysfunction and DNA damage.

L-Carnitine (CA; β-hydroxy-γ-trimethyl ammonium butyrate), a constituent of plasma and tissues, is biosynthesized in liver from lysine and methionine. It is essential for the transport free fatty acids into mitochondrial matrix for subsequent β-oxidation. CA has effects on glucose metabolism that has been related to its ability to stimulate FFA transport and oxidation in the mitochondria. This would restore the intramitochondrial acyl-CoA/CoA ratio which inturn promotes pyruvate dehydrogenase activity and hence glucose oxidation (Broderick et al., 1992). In an earlier study, we noted that CA attenuates insulin resistance in this animal model (Rajasekar et al., 2005). Further, the hepatoprotective effect of CA has been proved in adriamycin stress (Zeidan et al., 2002). Considering the foregoing observations the present study was designed to investigate the impact of CA on liver tyrosine phosphorylation status, expression of PKC βII, oxidative modification of proteins, nuclear

DNA staining and histology in this acquired model of syndrome X.

Materials and methods

Chemicals and drugs

L-Carnitine (CA) was obtained from the Sisco Research Laboratories (P) Ltd., Mumbai, India. Kit for protein tyrosine kinase (PTK) and PKC βII antibody were purchased from Sigma Chemical Company, MO, USA. All other chemicals and solvents were of analytical grade and were purchased from Himedia Laboratories Pvt. Ltd., Mumbai, India. Monoclonal antibodies against 4-hydroxy 2-nonenal (4-HNE), 2,4-dinitrophenol (DNP) and 3-nitrotyrosine (3-NT) were obtained as generous gift from Prof. Luke I. University of Oklahoma Health Sciences Centre, Prof. Ira Mellman, Yale University School of Medicine and Prof. Dick Lightfoot, Children's Hospital of Philadelphia.

Animals and treatment

Adult male Wistar rats of body weight ranging from 150 to 160 g were obtained from the Central Animal House, Rajah Muthiah Medical College, Annamalai University. They were housed in an animal room under controlled conditions on a 12 h light/12 h dark cycle. Animals received a standard pellet diet (Karnataka State Agro Corporation Ltd., Agro feeds division, Bangalore, India) and water ad libitum. The experimental procedures were ethically cleared and approved by the Institutional Ethical Committee of Animal Care, Rajah Muthiah Medical College, Annamalai University.

The animals were divided into four groups and were maintained as follows:

Group 1 (CON)–Control animals received the control diet containing starch and tap water ad libitum.
Group 2 (FRU)–Fructose-fed animals received the high fructose diet and water ad libitum.
Group 3 (FRU + CA)–Fructose-fed animals received the high fructose diet and CA (300 mg/kg/day, i.p).
Group 4 (CON + CA)–Control animals received the control diet and CA (300 mg/kg/day, i.p).

The diet composition is given in Table 1. The animals were maintained in their respective groups for 60 days. Body weights of animals were recorded. On day 59, 6 rats from each group were fasted overnight, anaesthetized with an intramuscular injection of ketamine hydrochloride (30 mg/kg) and sacrificed by cervical dislocation. Blood samples were collected and plasma was separated by centrifugation and glucose concentration was quantified by glucose oxidase method using kit (Qualigens Company, Mumbai). Plasma insulin was estimated by microparticle enzyme immuno assay method, using reagent kit (Boehringer Mannheim, Germany). Insulin levels were expressed as μU/ml. Homeostasic model assessment (HOMA), as a measure of insulin resistance was calculated using the formula: (insulin μU/ml × glucose mmol/l/22.5) (Mathews et al., 1985).

Table 1. Composition of diet (g/100 g)

Ingredients	Control diet	High fructose diet
Corn starch	60.0	–
Fructose	–	60.0
Casein (fat free)	20.0	20.0
Methionine	0.7	0.7
Groundnut oil	5.0	5.0
Wheat bran	10.6	10.6
Salt mixture*	3.5	3.5
Vitamin mixture**	0.2	0.2

* The composition of mineral mix (g/kg): $MgSO_4 \cdot 7H_2O$ – 30.5; NaCl – 65.2; KCl – 105.7; KH_2PO_4 – 200.2; $MgCO_3$ – 3.65; $Mg(OH)_2 \cdot 3H_2O$ – 38.8; Fe $C_6H_5O_7 \cdot 5H_2O$ – 40.0; $CaCO_3$ – 512.4; KI – 0.8; NaF – 0.9; $CuSO_4 \cdot 5H_2O$ – 1.4; $MnSO_4$ – 0.4 and $CONH_3$ – 0.05

** One kilogram of vitamin mix contained thiamine mono nitrate, 3 g; riboflavin, 3 g; pyridoxine HCl, 3.5 g; nicotinamide, 15 g; d-calcium pantothenate, 8 g; folic acid, 1 g; d-biotin, 0.1 g; cyanocobalamin, 5 mg; vitamin A acetate, 0.6 g; α-tocopherol acetate, 25 g and choline chloride, 10 g

PTK and PTP assays

All procedures were performed at 4 °C. Liver tissue was stimulated with insulin by opening the abdomen cavity and exposing the portal vein by injecting 10^{-5} mol/l insulin. Within 30 sec, the liver was removed, weighed and collected in ice-cold homogenisation buffer and homogenised at the maximum speed to remove the cell debris and nuclei. The supernatant collected was centrifuged for 1 h at 10,000 × *g* and the clear supernatant obtained was used for the assay of PTK.

The procedure was based on the detection of phosphorylated tyrosyl residues in an artificial substrate, poly-Glu-Tyr (PGT), using monoclonal anti-phosphotyrosine peroxidase conjugate. Color was developed with horseradish peroxidase chromogenic substrate, orthophenylenediamine and was read by spectrophotometry (ELISA reader) at 492 nm. The absorbance reflected the relative amount of tyrosine kinase activity in the samples.

For PTP assay, liver tissue was stimulated with insulin by opening the abdomen and exposing the portal vein by injecting 10^{-5} mol/l insulin. Within 30 sec, the liver sample was removed, minced coarsely with the buffer. The tissue homogenate was prepared with Tris–EDTA-sucrose (TES) buffer and then centrifuged at 400 × *g*, 4 °C to sediment nuclei. An aliquot of the tissue homogenate (0.05 ml) was added to 450 μl of reaction mixture which contained 50 mM morpholino ethane sulphonic acid, 150 mM NaCl, 2.5 mM EDTA, 0.1% bovine serum albumin, 2 mM dithiothreitol and 50 mM p-nitro phenyl phosphate and incubated for 10 min at 30 °C. The reaction was stopped by the addition of 500 ml of 2 M KOH and the amount of product (p-nitrophenol) produced was measured by determining the absorbance at 405 nm in a spectrophotometer. Nonspecific absorbance was corrected for by subtracting the absorbance at 405 nm determined in the absence of tissue homogenate. p-Nitrophenol (5–25 mmol) was used as the standard (Chen et al., 1997). Values were expressed as millimoles of p-nitrophenol liberated/min/mg protein.

PKC βII analysis

Liver tissue was rapidly dissected and washed with ice-cold phosphate buffered saline. PKC was partially purified from liver. Briefly, the samples were homogenized at 4 °C in buffer A (20 mM Tris–HCl buffer, pH 7.5, containing 0.33 M sucrose, 0.5 mM ethylene glycol tetra acetic acid (EGTA), 2 mM ethylene diamine tetra acetic acid (EDTA), 1 mM phenyl methyl sulphonyl fluoride (PMSF), 25 μg/ml leupeptin, 0.1 mg/ml aprotinin). The homogenates were centrifuged at 1000 × *g* for 10 min and the supernatant was ultracentrifuged at 1,00,000 × *g* for 30 min at 4 °C. The resulting supernatant was retained as the cytosolic fraction. The pellet was washed and resuspended with buffer B (Buffer A without sucrose) and homogenized again. The homogenates were solubilized in buffer B with 1% Triton X-100. After keeping it in ice for 45 min, the contents were centrifuged in an ultracentrifuge 1,00,000 × *g* for 30 min and the supernatant was labeled as the membrane fraction. Protein determination was performed according to the method of Lowry et al. (1951).

Immunoblot analysis

The supernatants containing equal amount of protein (100 μg) were separated on 10% SDS polyacrylamide gel electrophoresis (SDS-PAGE).

The proteins were transferred onto a nitrocellulose membrane (Hybond C+, Amersham Life Sciences) at 100 V for 30 min. Membrane was then washed thrice with PBS and blocked overnight in Tris buffered saline-Tween 20 (TBTS: 20 mM Tris, 500 mM NaCl and 0.1% Tween 20) buffer. Then, the membrane was incubated with primary antibody (mouse monoclonal anti-protein kinase C βII at a dilution 1:1000) in TBST buffer containing 1% non-fat dry milk and agitated gently at 4 °C overnight. The membrane was washed thrice with PBS for 5 min. Secondary antibody (anti-mouse) in PBS containing 1% BSA and 0.1% Tween-20 was allowed to hybridize for 2 h at room temperature. The bands were detected by enhanced chemiluminescence technique (ECL) using super signal ECL kit from Pierce technology. The band intensity was quantified using a densitometer (Bio Rad-GS710).

Histology and immunohistochemistry

Four animals from each group were anesthetized using light ether, perfused with 10% formalin and the liver tissue was separated and placed in formalin. They were later sectioned using a microtome, dehydrated in graded alcohol, embedded in paraffin section. Lipid accumulation was assayed by staining the section with hemotoxylin and eosin. For immunohistochemistry 4 μm paraffin sections were deparaffinized with xylene and rehydrated with graded concentrations of isopropyl alcohol. Sections were incubated with peroxide blocking reagent for 10 min, rinsed with phosphate buffer and again incubated with power block solution for ten minutes. Non-specific binding was minimized by leaving the sections in 3% BSA in phosphate buffered saline for 30 min. Sections were incubated overnight with 1:700 dilution of anti-3NT antibody or with 1:500 dilution of anti-DNP antibody or with 1:100 dilution of anti-4-HNE antibody. The sections were rinsed well with phosphate buffer and incubated with super enhancer reagent for 30 min. After rinsing with phosphate buffer, incubation was done with super sensitive polymer-horseradish peroxidase immunohistochemistry detection system (Biogenex laboratories). After washing thoroughly with phosphate buffer, the sections were incubated with diaminobenzidene substrate solution for 5 min. Sections were counterstained with hematoxylin and observed under light microscopy. All the sections from the various groups were incubated under the same conditions with similar antibody concentration, and in the same running in order to make the immunostaing comparable among the different experimental groups.

Hepetocyte isolation and PI staining

Rats were fasted for 24 h prior to hepatocyte isolation. The rats were anesthetized with ketamine hydrochloride (30 mg/kg) intramuscularly and hepatocytes were isolated according to the method of Seglen (1976). Hepatocytes were washed in PBS thrice and incubated for another 10 min with 50 μl of propidium iodide (5 mg/ml) and examined by fluorescence microscopy after mounting (Olympus BX51). Quantification of data was obtained by examination of a defined area of each slide.

Statistical analysis

Values are expressed as means ± SD. Data within the groups are analyzed using one-way analysis of variance followed by Duncan's multiple range test. A value of $p < 0.05$ was considered statistically significant.

Results

The mean final body weights of animal groups were as follows (CON: 179.5 ± 4.65 g, FRU: 195.7 ± 5.47 g, FRU + CA: 188.66 ± 4.19 g, CON ± CA: 178.35 ± 5.38 g) Weight gain was observed in all the groups, which did not significantly vary between the groups.

The fructose-fed rats (group 2) developed hyperinsulinemia and hyperglycemia which were prevented in CA administered fructose-fed rats [Glucose (mg/dl) CON: 76.83 ± 4.87; FRU: 125.83 ± 4.05; FRU + CA: 78.16 ± 4.87 and CON + CA: 74.41 ± 4.05; insulin (μU/ml) CON: 44.43 ± 3.28; FRU: 82.73 ± 5.62; FRU + CA: 46.27 ± 4.28 and CON + CA: 44.39 ± 3.02]. The degree of insulin resistance as calculated by HOMA was high in fructose-fed rats [CON: 8.41 ± 0.61; FRU: 25.64 ± 1.20; FRU + CA: 8.92 ± 0.82; CON + CA: 8.71 ± 0.71]. HOMA values were not significantly different between CA treated

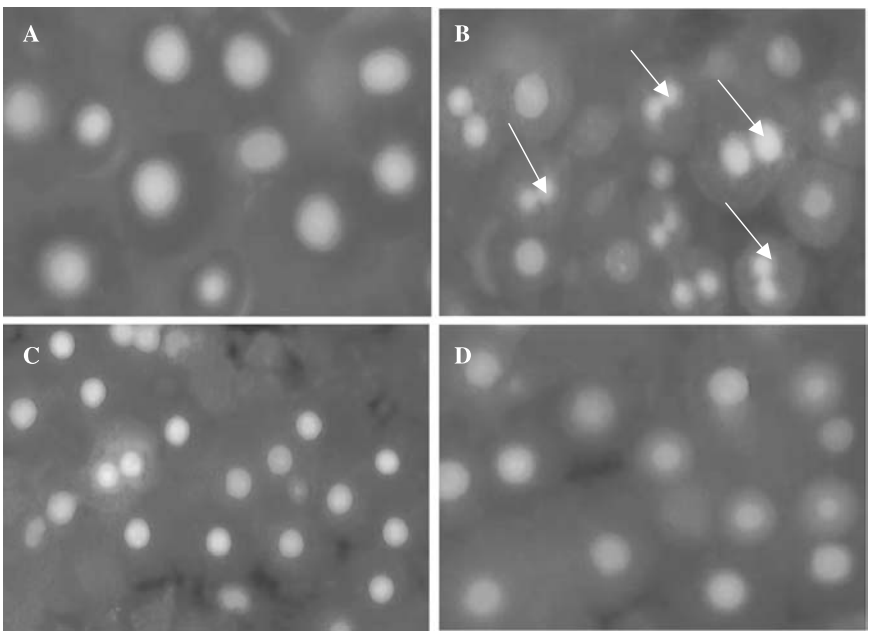

Fig. 1. **A** Control rat hepatocytes with normal nuclei. **B** Fructose-fed rat hepatocytes. Arrows show apoptotic cells with fragmented nuclei. **C** CA treated hepatocytes with reduced apoptotic nuclei. **D** CA treated control rat hepatocytes with similar normal morphology

rats and control rats. Fructose-fed rats displayed a rise in FFA which was prevented by CA [free fatty acid (mg/dl) CON: 91.25 ± 6.30; FRU: 125.45 ± 9.61; FRU + CA: 95.14 ± 5.53; CON + CA: 88.56 ± 7.21].

Hepatocytes isolated from fructose-fed untreated rats showed more apoptotic nuclei (Fig. 1B) as compared to control animals after PI staining (Fig. 1A). Formation of apoptotic bodies was found to be reduced in CA-treated rats (Fig. 1C). Hepatocytes from control rats treated with CA displayed normal (Fig. 1D) nuclei as that of control.

Figure 2 represents the PTP activity in liver of control and experimental animals. PTP activity was significantly increased in liver of fructose-fed rats as compared to that of control rats. CA administered fructose-fed rats showed significant reduction in the activity of PTP as compared to untreated fructose-fed rats. No significant alterations were observed in control rats treated with CA.

Figure 3 is a bar diagram depicting the relative absorbance of samples at 405 nm, as an index of PTK activity in liver of control and experimental animals. PTK activity

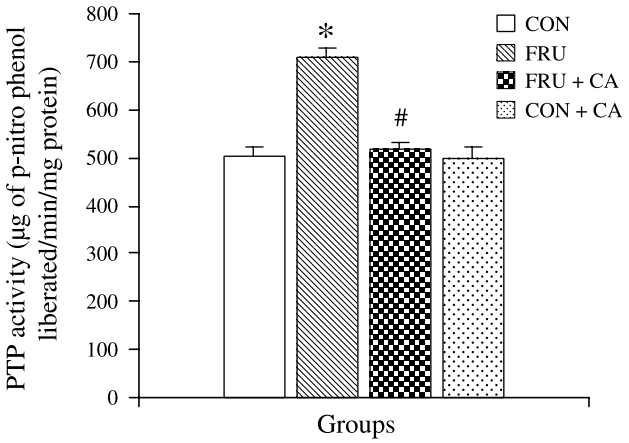

Fig. 2. Protein tyrosine phosphatase activity of experimental animals. Values are means ± SD; $n = 6$. *Significant as compared to control rats. #Significant as compared to fructose-fed rats. ANOVA followed by DMRT; $p < 0.05$

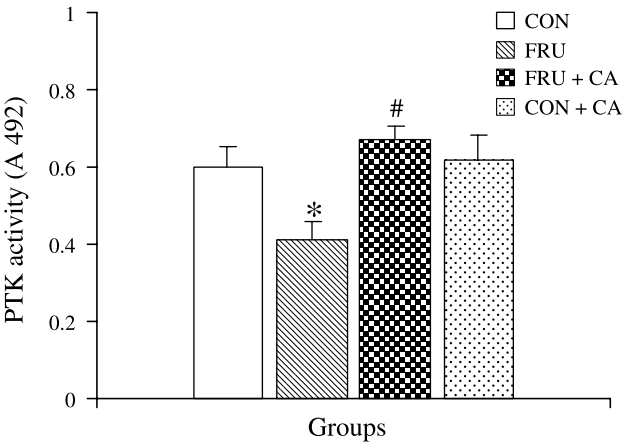

Fig. 3. Protein tyrosine kinase activity of experimental animals. Values are means ± SD; $n = 6$. *Significant as compared to control rats. #Significant as compared to fructose-fed rats. ANOVA followed by DMRT; $p < 0.05$

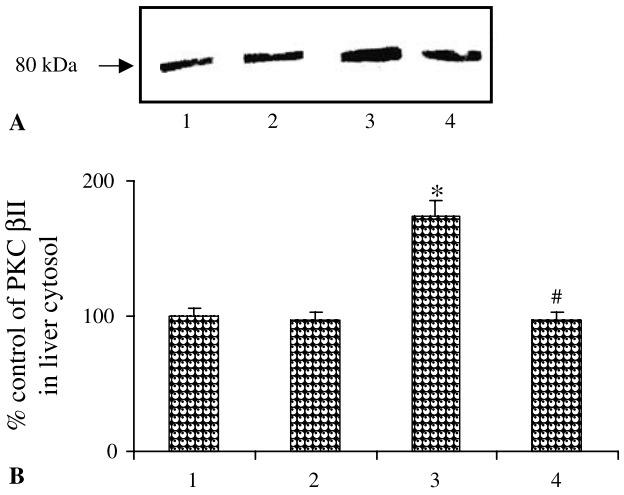

Fig. 4. Representative immunoblots showing increased expression of PKC βII isoenzyme in liver cytosol. **A** Densitometry analysis of Western blot. Data are expressed as percentage of control and are means ± SD of six independent measurements. **B** *1* CON; *2* CON + CA; *3* FRU; *4* FRU + CA. *Significant as compared to CON. #Significant as compared to FRU. ANOVA followed by DMRT; $p < 0.05$

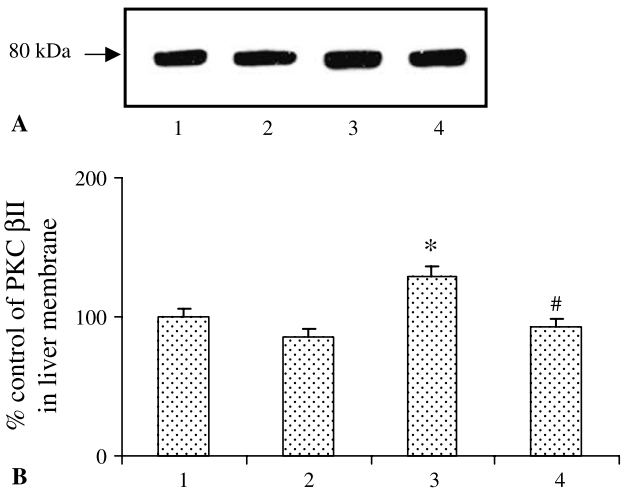

Fig. 5. Representative immunoblots showing increased expression of PKC βII isoenzyme in liver membrane. **A** Densitometry analysis of Western blot. Data are expressed as percentage of control and are means ± SD of six independent measurements. **B** *1* CON; *2* CON + CA; *3* FRU; *4* FRU + CA. *Significant as compared to CON. #Significant as compared to FRU. ANOVA followed by DMRT; $p < 0.05$

was significantly decreased in liver of fructose-fed rats as compared to that of control rats. CA treated fructose-fed rats showed a significant increase in the activity as compared to fructose-fed rats, while CA-treated control rats showed no significant changes in activity as compared to control rats.

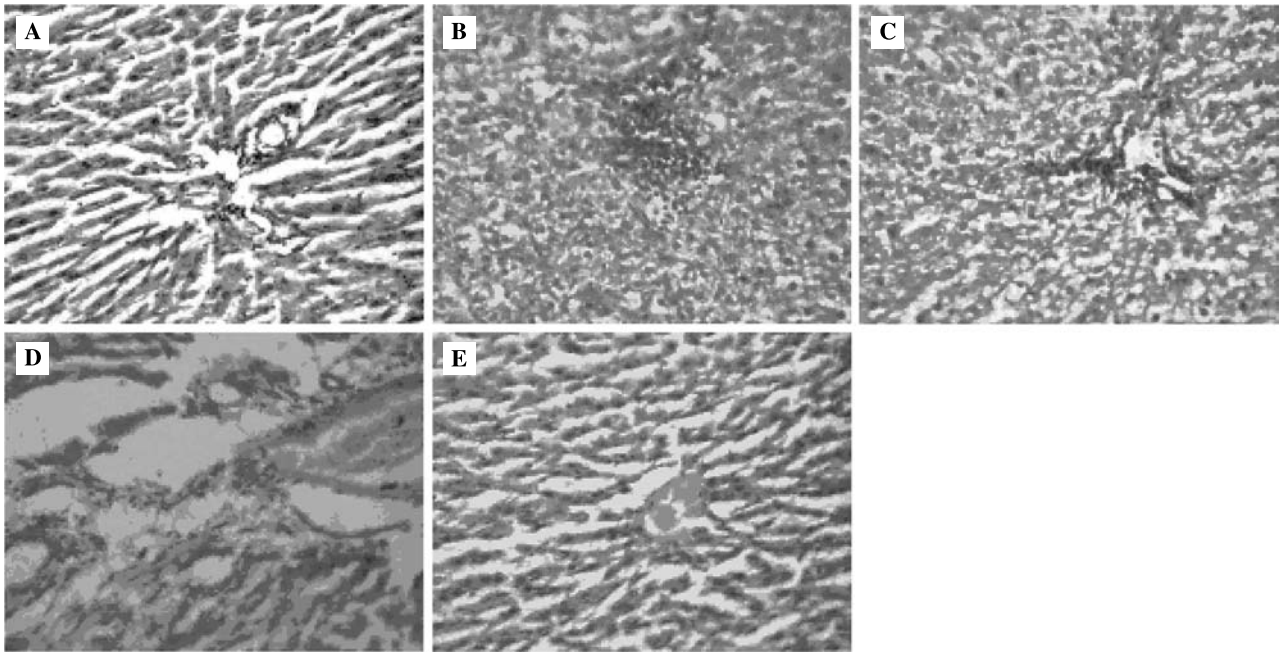

Fig. 6. **A** Liver of control rats. H&E ×20. Portal triad and hepatocytes are within normal limits. **B** Liver of fructose-fed rat. H&E ×20. Microvascular type of fatty changes. Focal Kupffer cell hyperplasia. **C** Liver of fructose-fed rats. H&E ×20. Shows inflammatory cells infiltration around the portal triad. **D** Liver of CA administered fructose-fed rat. H&E ×20. Reduced fatty changes and congestion of central vein. Hepatocytes are within normal limits. **E** Liver of CA administered control rats. H&E ×20. Hepatocytes are within normal limits and central vein shows congestion

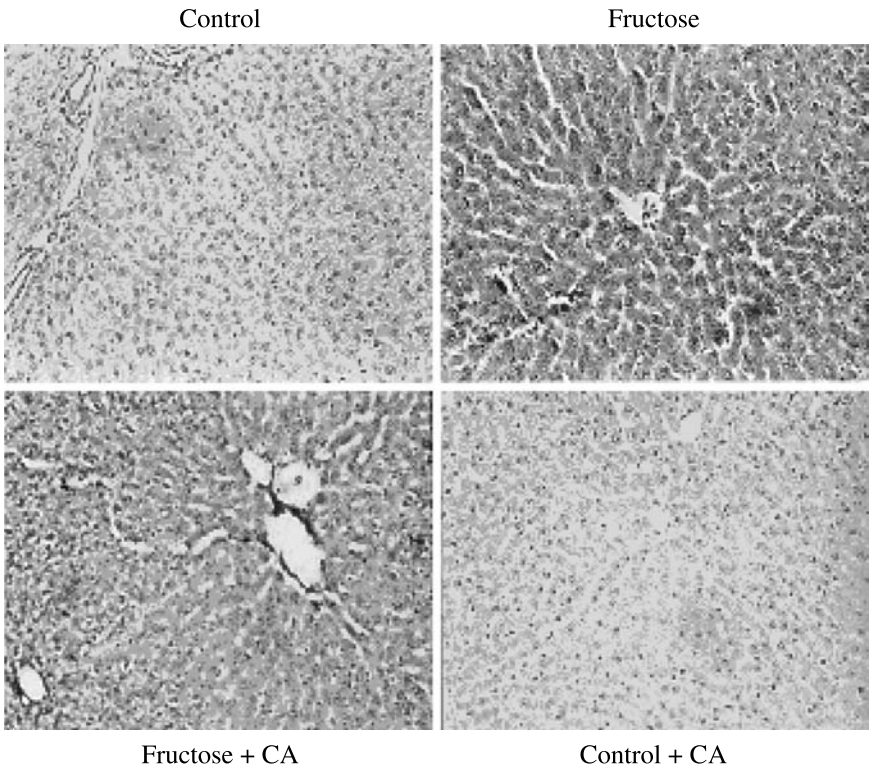

Fig. 7. Immunohistochemistry for 4-hydroxynonenal (HNE) protein adduct. HNE immunostaining is increased in liver of fructose-fed animal and is markedly decreased in CA-treated fructose-fed animal. Both control and CA-treated control animals show negative staining for this antibody (40×)

Figures 4 and 5 depict the expression of PKC βII in the liver cytosolic and membrane fractions respectively. The protein expression was significantly increased in the both cytosolic and membrane fractions in FRU as compared to control animals. Expression was significantly reduced in the both fractions of the CA treated fructose-fed animals.

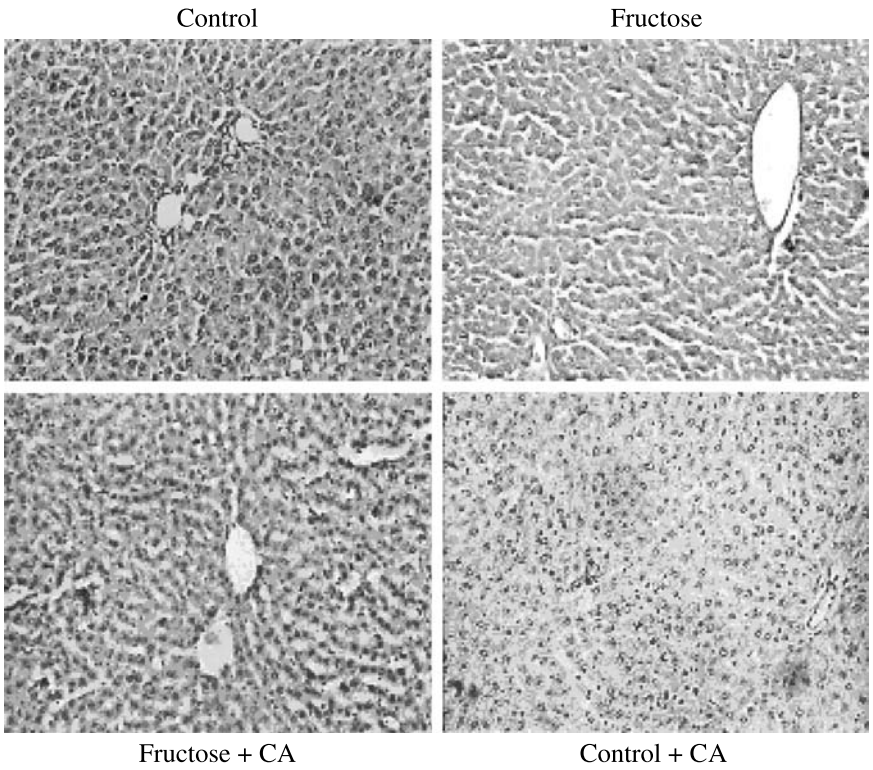

Fig. 8. Immunohistochemistry for 2,4-dinitrophenol (DNP) modified protein. DNP immunostaining is increased in liver of fructose-fed animals and is reduced in CA-treated fructose-fed animals. Both control and CA-treated control animals show negative staining for this antibody (40×)

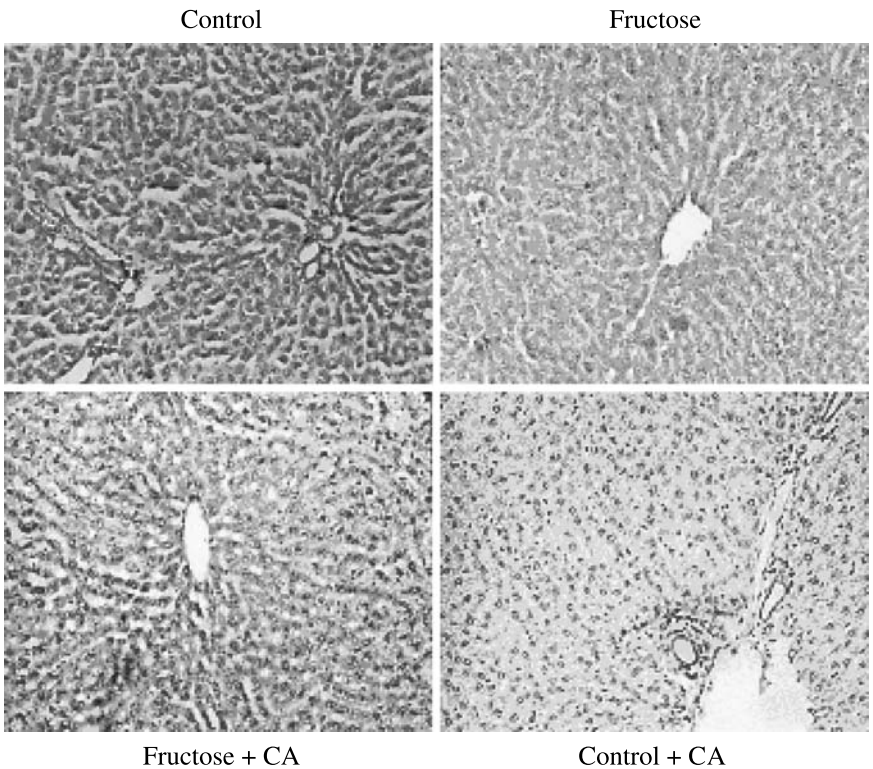

Fig. 9. Immunohistochemistry for 3-nitrotyrosine (3-NT) protein adduct in liver. 3-NT immunostaining is intense in liver of fructose-fed animals and is reduced in CA-treated fructose-fed animal. Both control and CA-treated control animals show negative staining for this antibody (40×)

Normal rats treated with CA also appeared to show reduced expression of PKC βII, which however, was not statistically significant.

Histopathological analysis of the liver sample from fructose-fed rat depicts increased microvascular type of fatty changes, and focal Kupffer cell hyperplasia (Fig. 6B) and inflammatory cell infiltration around the portal triad (Fig. 6C). These changes were abolished upon CA treatment. The CA administered fructose-fed rat showed reduced fatty changes and the hepatocytes were within normal limits. CA treated control rats showed a normal pattern.

Figures 7, 8 and 9 represent the photomicrographs on the accumulation of 4-HNE, DNP and 3-NT adducts in liver of experimental rats. The intensity of 4-HNE, DNP and 3-NT staining were more pronounced in fructose-fed rat liver than in controls. It is worthy to note that there was a marked reduction in 4-HNE, DNP and 3-NT immunoreactivity in the liver of rats treated with CA. There was no apparent difference in the immunoreactivity for these antibodies in liver of control rat treated with CA.

Discussion

Many studies have reported the aberrant regulation of insulin signaling pathways in this diet-induced rat model of insulin resistance (Bezerra et al., 2000; Ueno et al., 2000; Catena et al., 2003). Recent insights into the mechanism of insulin action have demonstrated that reversible tyrosine phosphorylation of the insulin receptor and its cellular substrate proteins play a crucial role in its action. Insulin signaling is initiated by binding of insulin to the extracellular α-subunit of insulin receptor, resulting in the stimulation of β-subunit, which contains intrinsic receptor tyrosine kinase activity and autophosphorylation of the receptor at multiple tyrosine residues. This event enhances the intrinsic tyrosine kinase activity and evokes a series of phosphorylation events. These include tyrosyl phosphorylation of intracellular substrates named insulin receptor substrates (IRS 1–4) and other molecules. The phosphorylated proteins mediate the cellular actions of insulin. PTP are the enzymes responsible for the selective dephosphorylation of tyrosine residues. The extent of tyrosyl phosphorylation on a given protein is controlled by the reciprocal actions of PTK and PTP activities. The decrease in phosphorylation status observed in the current study may be of biological importance because a reduction in receptor phosphorylation has been correlated with insulin resistance in different animal models (Carvalho et al., 1996). Taghibiglou et al. (2002) have suggested that hepatic insulin resistance induced by high fructose feeding in part could be attributed to upregulation PTP-1B (a non-transmembrane PTP).

Serine/threonine phosphorylation of the signaling proteins could be yet another reason for reduced tyrosine phosphorylation of proteins. The insulin receptor substrates contain many potential serine/threonine phosphorylation sites in motifs recognized by various kinases such as PKC, and mitogen-activated protein kinases (Mothe and Van, 1996). PKC has been shown to serine/threonine eonine phosphorylate both the insulin receptor on the β-subunit particularly on serine residue 994 and 1023/25 and IRS1 (Chin et al., 1992; Ravichandran et al., 2001), leading to decreased autophosporylation and increased receptor degradation. We observed an increased activity of the βII isoform. Taken together, it is possible that in insulin resistant rats the elevation in PKC activity, by increasing serine phosphorylation might block tyrosine phosphorylation.

The enhanced tyrosine phosphorylation status following insulin stimulus in CA-treated rat liver suggest phosphorylation of β-subunit and further components of insulin signaling cascade and is indicative of an insulin potentiating action of CA. Mechanisms relating to enhanced tyrosine phosphorylation are not clear but a study has shown that pro-and antioxidative metabolites can differentially regulate PTP (McClung et al., 2004). PTP contains a cysteine residue at the active site that plays a regulatory role in its catalytic process of tyrosine dephosphorylation (Fauman and Saper, 1996). Further, glutathionylation of the enzyme protein may modulate its activity. For instance, a shift in the glutathione-redox pair to a more oxidized state is the driving force for the increased expression of PTP-1B (Muller and Pallauf, 2006). Considering these observations we speculate that CA, by restoring the redox state of the cell may alter the critical cysteine and inactivate PTP causing a sustained increase in protein tyrosine phosphorylation. Additionally neutralization of ROS and maintenance of intracellular redox balance could contribute to a blockade of stress sensitive kinases and activation of tyrosine phosphorylation. This corresponded well with the replenishment of glutathione by CA, reported earlier in this model (Rajasekar et al., 2005).

Isoform-selective protein kinase (PKC τ) increases have been observed in white muscle in this model of IR associated with a rise in diacylglycerol (DAG) (Donnelly et al., 1994). Activation of DAG–PKC pathway in liver tissue may compromise cellular function and is recognized as a causative factor in the pathogenesis of diabetic

complications. It is clear that increase in PKC through the glucose-induced DAG formation is an important mechanism of glucose toxicity in fructose-fed rats. CA may reduce glucose level in cells and interfere with DAG formation from glucose (de novo synthesis) or from membrane phopholipid hydrolysis. It is of importance to note that CA regulates hepatic glucose metabolism and suppresses glucose overproduction in these animals (Rajasekar and Anuradha, 2007).

Activation of PKC is sensitively regulated through redox changes in sulfhydryl group of cysteine-rich regions in the protein (Gschwendt et al., 1991). Antioxidants including vitamin E and taurine suppressed glucose-induced rise in PKC (Studer et al., 1997). Thus in addition to glucose lowering effect, the antioxidant function of CA reduces the level of cellular oxidants and might protect reactive protein sulfhydryl of PKC from oxidation.

The rats fed fructose displayed micro- and macro-vascular type of fatty changes in liver indicating the lipogenic state. Kupffer cell hyperplasia and inflammatory cell infiltration around portal triad can activate deleterious stress-sensitive pathways and compromise cellular function (Kelley et al., 2004). This condition involving accumulation of fats in insulin sensitive tissues associated with impairment in insulin action has been described as ''lipotoxicity'' which is mediated essentially by the products such as free fatty acids, ceramide and DAG.

Histological localization of 4-HNE, 3-NT and DNP adducts provide evidence for oxidative damage in liver of the fructose-fed rats. HNE is one of the most abundant and highly toxic lipid aldehydes which has cytopathologic effects by its strong reactivity with biomolecules (Uchida, 2003). 3-NT and DNP adducts are formed by the reaction of reactive nitrogen species (RNS) with proteins (Szabo, 2003). Tyrosine nitration can prevent the phosphorylation and dimerization of tyrosine, an important step for signal transduction (Ischiropoulos, 1998).

Decreased immunostaining in CA treated rats suggest that CA itself may be able to scavenge in vivo ROS and RNS involved in the process. CA has favorable structure-function configuration by the presence of hydroxyl and carboxylate groups essential for chelation of Fe^{2+} ions and antixodiation (Gulcin, 2006). Further, CA, by virtue of its ability to enhance ATP production could reduce susceptibility to oxidative damage. Supplementation of CA may spare vitamin C, an important antioxidant and essential cofactor for biosynthesis of CA.

Elevation of glucose and FFA in cells could contribute to apoptosis of hepatocytes form fructose-fed rats. High-glucose induced apoptosis was found in cultured human umbilical vein endothelial cells and in proximal tubular cells of rats infused with 10% glucose (Ishii et al., 1996). Long-term exposure to FFA (100–300 μmol/l) for 24 h has been shown to trigger apoptosis in human endothelial cells (Artwohl et al., 2004). Long-chain FFA are hydrophobic anions that exhibit properties similar to those of anionic detergents. They interact with voltage-dependent anion channels in mitochondria and induce membrane permeability transition and cytochrome C release, thereby activating caspases (Furuno et al., 2001). CA participates in cellular defence against apoptosis by acting as a GSH replenisher, by reducing FFA and ceramide (a promoter of apoptosis) and by regulation of caspases 3 and 8 (Mutomba et al., 2000).

Inhibitors of PTP (a negative modulator of insulin action) and PKC have the potential to improve insulin sensitivity and form a promising therapeutic strategy for diabetic complications. Our data suggest that CA holds great potential as a therapeutic regimen for insulin resistance.

Acknowledgment

The authors wish to thank the University Grant Commission, New Delhi, India, for providing financial support.

References

Artwohl M, Roden M, Waldhausl W, Freudenthaler A, Baumgartner-Parzer SM (2004) Free fatty acids trigger apoptosis and inhibit cell cycle progression in human vascular endothelial cells. FASEB J 18: 146–148

Bassienmaier B, Mosthab L, Mischak H, Ullrich A, Haring HU (1997) Protein kinase C isoform beta-1 and beta-2 inhibit the tyrosine kinase activity of the insulin receptor. Diabetologia 40: 863–866

Bezerra RM, Ueno M, Silva MS, Tavares DQ, Carvalho CR, Saad MJ (2000) A high fructose diet affects the early steps of insulin action in muscle and liver of rats. J Nutr 130: 1531–1535

Broderick TL, Quinney HA, Lopaschuk GD (1992) Carnitine stimulation of glucose oxidation in the fatty acid perfused isolated working rat heart. J Biol Chem 267: 3758–3763

Carvalho CR, Brenelli SL, Silva AC, Nunes AL, Velloso LA, Saad MJ (1996) Effect of aging on insulin receptor, insulin receptor substrate-1, and phosphatidylinositol 3-kinase in liver and muscle of rats. Endocrinology 137: 151–159

Catena C, Giacchetti G, Novello M, Colussi G, Cavarape A, Sechi LA (2003) Cellular mechanisms of insulin resistance in rats with fructose-induced hypertension. Am J Hypertens 16: 973–978

Chen H, Wertheimer SJ, Lin CH, Katz SL, Amrein KE, Burn P, Quon MJ (1997) Protein-tyrosine phosphatases PTP1B and syp are modulators of insulin-stimulated translocation of GLUT4 in transfected rat adipose cells. J Biol Chem 272: 8026–8031

Chin JE, Dickens M, Tavare JM, Roth RA (1992) Overexpression of protein kinase C isoenzymes alpha, beta I, gamma, and epsilon in cells overexpressing the insulin receptor. Effects on receptor phosphorylation and signaling. J Biol Chem 268: 6338–6347

Donnelly R, Reed MJ, Azhar S, Reaven GM (1994) Expression of the major isoenzyme of protein kinase-C in skeletal muscle, nPKC theta,

varies with muscle type and in response to fructose-induced insulin resistance. Endocrinology 135: 2369–2374

Fauman EB, Saper MA (1996) Structure and function of the protein tyrosine phosphatases. Trends Biochem Sci 21: 413–417

Faure P, Rossini E, Lafond JL, Richard MJ, Favier A, Halimi S (1997) Vitamin E improves the free radical defense system potential and insulin sensitivity of rats fed high fructose diets. J Nutr 127: 103–107

Furuno T, Kanno T, Arita K, Asami M, Utsumi T, Doi Y, Inoue M, Utsumi K (2001) Roles of long chain fatty acids and carnitine in mitochondrial membrane permeability transition. Biochem Pharmacol 62: 1037–1046

Gschwendt M, Kittstein W, Marks F (1991) Protein kinase C activation by phorbol esters: do cysteine-rich regions and pseudosubstrate motifs play a role? Trends Biochem Sci 16: 167–169

Gulcin I (2006) Antioxidant and antiradical activities of L-carnitine. Life Sci 78: 803–811

Ischiropoulos H (1998) Biological tyrosine nitration: a pathophysiological function of nitric oxide and reactive oxygen species. Arch Biochem Biophys 356: 1–11

Ishii N, Ogawa Z, Suzuki K, Numakami K, Saruta T, Itoh H (1996) Glucose loading induces DNA fragmentation in rat proximal tubular cells. Metabolism 45: 1348–1353

Kelley GL, Allan G, Azhar S (2004) High dietary fructose induces a hepatic stress response resulting in cholesterol and lipid dysregulation. Endocrinology 145: 548–555

Lowry OH, Rosebrough NJ, Farr AL, Randall RJ (1951) Protein measurement with the Folin's – phenol reagent. J Biol Chem 193: 265–275

Mathews DR, Hosker JP, Rudenkl AS, Naylor BA, Treacher DF, Turner RC (1985) Homeostasis model assessment: insulin resistance and β-cells function from fasting plasma glucose and insulin concentrations in man. Diabetologia 28: 412–419

McClung JP, Roneker CA, Mu W, Lisk DJ, Langlais P, Liu F, Lei XG (2004) Development of insulin resistance and obesity in mice over expressing cellular glutathione peroxidase. Proc Natl Acad Sci USA 101: 8852–8857

Miwa I, Ichimura N, Sugiura M, Hamada Y, Taniguchi S (2000) Inhibition of glucose-induced insulin secretion by 4-hydroxy-2-nonenal and other lipid peroxidation products. Endocrinology 141: 2767–2772

Mothe I, Van OE (1996) Phosphorylation of insulin receptor substrate-1 on multiple serine residues, 612, 632, 662, and 731, modulates insulin action. J Biol Chem 271: 11222–11227

Mueller AS, Pallauf MJ (2006) Compendium of the antidiabetic effects of supranutritional selenate doses. In vivo and in vitro investigations with type II diabetic db/db mice. J Nutr Biochem 17: 548–560

Mutomba MC, Yuan H, Konyavko M, Adachi S, Yokoyama CB, Esser V, McGarry JD, Babior BM, Gottlieb RA (2000) Regulation of the activity of caspases by L-carnitine and palmitoylcarnitine. FEBS Lett 478: 19–25

Rajasekar P, Kaviarasan S, Anuradha CV (2005) L-Carnitine administration prevents oxidative stress in high fructose-fed insulin resistant rats. Diabetol Croat 34: 21–28

Rauen U, Polzar B, Stephan H, Mannherz HG, de GH (1999) Cold-induced apoptosis in cultured hepatocytes and liver endothelial cells: mediation by reactive oxygen species. FASEB J 13: 155–168

Ravichandran V, Esposito DL, Chen J, Quon MJ (2001) Protein kinase C-zeta phosphorylates insulin receptor substrate-1 and impairs its ability to activate phosphatidylinositol 3-kinase in response to insulin. J Biol Chem 276: 3543–3549

Reaven GM (1994) Syndrome X: 6 years later. J Int Med 736: 13–22

Seglen PO (1976) Preparation of isolated rat liver cells. Methods Cell Biol 13: 29

Studer RK, Craven PA, DeRubertis FR (1997) Antioxidant inhibition of protein kinase C-signaled increases in transforming growth factor-beta in mesangial cells. Metabolism 46: 918–925

Szabo C (2003) Multiple pathways of peroxynitrite cytotoxicity. Toxicol Lett 140–141: 105–112

Taghibiglou C, Rashid-Kolvear F, Van Iderstine SC, Le-Tien H, Fantus IG, Lewis GF, Adeli K (2002) Hepatic very low density lipoprotein-ApoB overproduction is associated with attenuated hepatic insulin signaling and overexpression of protein tyrosine phosphatase 1B in a fructose-fed hamster model of insulin resistance. J Biol Chem 277: 793–803

Uchida K (2003) 4-Hydroxy-2-nonenal: a product and mediator of oxidative stress. Progr Lipid Res 42: 318–343

Ueno M, Bezerra RM, Silva MS, Tavares DQ, Carvalho CR, Saad MJ (2000) A high-fructose diet induces changes in pp185 phosphorylation in muscle and liver of rats. Braz J Med Biol Res 33: 1421–1427

Zeidan Q, Strauss M, Porras N, Anselmi G (2002) Differential long-term subcellular responses in heart and liver to adriamycin stress. Exogenous L-carnitine in cardiac and hepatic protection. J Submicrosc Cytol Pathol 34: 315–321

Authors' address: Prof. Dr. C. V. Anuradha, Department of Biochemistry and Biotechnology, Annamalai University, Annamalai Nagar 608 002, Tamil Nadu, India,
E-mail: cvaradha@hotmail.com